25th ABCM International Congress of Mechanical Engineering
October 20-25, 2019, Uberlândia, MG, Brazil

COB-2019-2084
STUDY ABOUT FINITE ELEMENT PLATES BASED ON THE REISSNER-MINDLIN THEORY

Jefferson da Silva Carvalho
Roque Luiz da Silva Pitangueira
Universidade Federal de Minas Gerais (UFMG). Av. Antônio Carlos, 6627, Pampulha. Belo Horizonte – Minas Gerais
jeffersondsc@outlook.com ; roque@dees.ufmg.br

Abstract. *This paper is intended as a numerical quali-quantitative study of convergence, spurious modes and computing time for thin and thick plate elements, under full and reduced integration, with basis on Reissner-Mindlin plate theory. Simulations have been run using the INSANE system. From the convergence results, a good performance of reduced integration in the thin plate is noticed, especially when a Q4 element is introduced, along with a new way to solve the shear locking in this case of thickness, by using full integration with elements of higher order and small dimensions. In the thick plate, reduced integration with refined mesh and lower order elements, such as Q4 and Q9, is also an alternative in cases in which higher order elements with full integration are not possible. Each one of these different possibilities of carrying out the same convergence analysis performs differently, in terms of spurious modes and time. It is possible to conclude that there is no ideal path in the analysis of plate finite elements. Therefore, a good balance between the two last parameters in the study becomes useful in making the best choice in every single simulation to be run.*

Keywords: *Reissner-Mindlin Plate, Finite Element Method, Shear Locking, Reduced Integration, Convergence*

1. INTRODUCTION

A plate structure is an important engineering component used in many industries, such as aerospace and civil engineering. According to Cen and Shang (2015), the Finite Element Method (FEM) is usually the most effective and convenient artifice for the analysis of these types of structures. The elements used to develop this method for plates are based on two main hypotheses: the Kirchhoff theory, used for thin plates only, and the Reissner-Mindlin theory, applicable for plates of any thickness. For an in-depth investigation on plate thicknesses, this work is intended as a study of finite elements with the latter assumptions as its foundation. Although a problem occurs when this theory is applied to thin plates, namely, the shear locking phenomenon mentioned in Soriano (2003), such problem can be overcome by using reduced integration, an anti-locking technique used in this work, even though it introduces spurious mechanisms.

As mentioned above, the study proposed is the aim of this paper. It comprises a convergence analysis and its spurious modes and computing time for thin and thick plates by using full and reduced integration.

2. FINITE ELEMENTS BASED ON REISSNER-MINDLIN PLATE THEORY

The assessment of convergence is based on the transverse displacement of a plate, under linear and static analysis. Consonant with Oñate (2013), the obtaining process for this variable in the FEM model starts from the displacement field of the Reissner-Mindlin mathematical model which is discretized into a mesh of *n* element nodes of the plate middle plane. Since this theory establishes the independency of the transverse displacement *w* and the two rotations θ_x and θ_y expressed on the vector $\{u\}$, these variables are interpolated using C^0 shape functions as written in Eq. (1).

$$\{u\}=\begin{Bmatrix} w \\ \theta_x \\ \theta_y \end{Bmatrix} = \sum_{i=1}^{n} \begin{Bmatrix} N_i w_i \\ N_i \theta_{x_i} \\ N_i \theta_{y_i} \end{Bmatrix} = [N]\,\{d\} \tag{1}$$

where $[N]$ and $\{d\}$ are the shape function matrix and the displacement vector for the element at a node i, in this order.

The shape functions of plate elements are known in Oñate (2009), but the displacement vector needs to be found. For this purpose, the Principle of Virtual Work (PVW) can be applied resulting in the element equilibrium equation as follows in Eq. (2).

$$[k]\{d\}=\{f_{eq}\}+\{p\} \tag{2}$$

where $\{p\}$ is the concentrated force vector and $[k]$ and $\{f_{eq}\}$ are the element stiffness matrix and the equivalent nodal force vector due to distributed loads, respectively, obtained according to Eq. (3) and Eq. (4), in this order.

$$[k]=\iint_A [B]^T\,[\widehat{D}]\,[B]\,dA \tag{3}$$

$$\{f_{eq}\}=\iint_A [N]^T\{q\}\,dA \tag{4}$$

In Equation (4), $\{q\}$ is the distributed forces vector and in Eq. (3), $[B]$ is the generalized strain matrix and $[\widehat{D}]$ is the generalized constitutive matrix of the material. To obtain Eq. (3) and Eq. (4) for shape functions in natural coordinate system ξ, η, with isoparametric and subparametric elements, and computing them with numerical integration by a Gauss quadrature, these formulas can be expressed as Eq. (5) and Eq. (6), respectively.

$$[k]=\sum_{i=1}^{p1}\sum_{j=1}^{p2} H_i H_j \left[[B]^T(\xi_i,\eta_j)\,[\widehat{D}]\,[B](\xi_i,\eta_j)\,\left|[J](\xi_i,\eta_j)\right|\right] \tag{5}$$

$$\{f_{eq}\}=\sum_{i=1}^{p1}\sum_{j=1}^{p2} H_i H_j \left[[N]^T(\xi_i,\eta_j)\,\{q\}\,\left|[J](\xi_i,\eta_j)\right|\right] \tag{6}$$

where $p1$ and $p2$ are the number of integration points in ξ and η directions, in this order, H_i and H_j the corresponding weights and $|[J]|$ is the Jacobian determinant.

3. METHODS

The study employs numerical simulations produced by the software INSANE (INteractive Structural ANalysis Environment), used for preprocessing the models and also for processing and postprocessing the displacement results and the spurious modes.

The models propose a square thin plate and a circular thick plate, both composed of homogeneous isotropic material with Young's modulus $E=1{,}092{,}000\ N/mm^2$ and Poisson's ratio $v=0.3$. Their dimensions are shown in Fig. 1 where the thin plate has a side $a=10\ mm$ and thickness $t=0.4\ mm$ and the thick plate has a radio $a=5mm$ and thickness $t=2mm$.

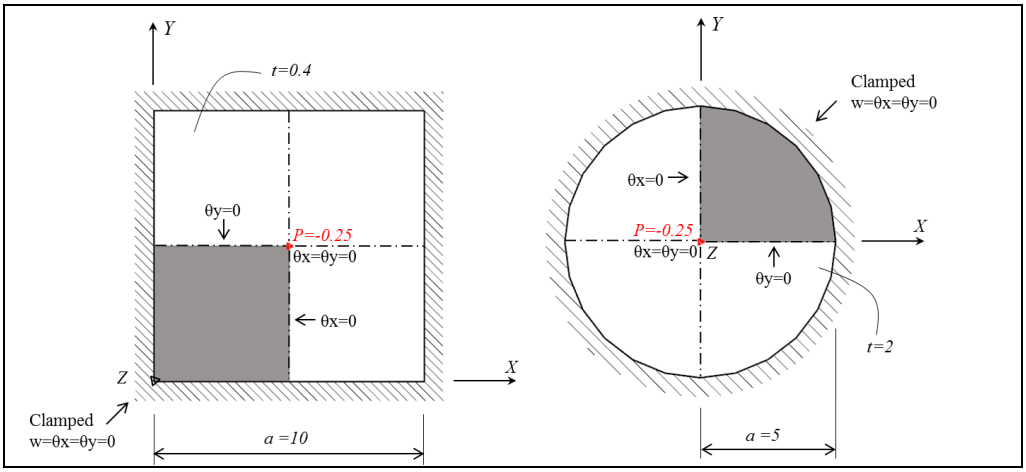

Figure 1. Dimensions (mm) of the plates and loads (N) and boundary conditions for 1/4 of the models.

The plates were clamped and under a central concentrated load in Z direction with magnitude $P= -1\ N$. Due to the double symmetry of the plates, only one quarter of the geometries and loadings were used according to the previous figure. Linear, quadratic and cubic Reissner-Mindlin quadrilateral plate elements of Lagrange family, Q4, Q9 and Q16 in this order, were assigned on the meshes.

In each model, the analysis of convergence was carried out under two integration conditions. The first one applied full integration (F) on the elements and assessed how convergence worked, especially in thin plates, without the anti-locking technique and proceeded by only increasing the degrees of freedom of the model. It was done by enhancing the element orders combined with their mesh refinement which followed the parameter in Fig. 2 described in Saliba (2007).

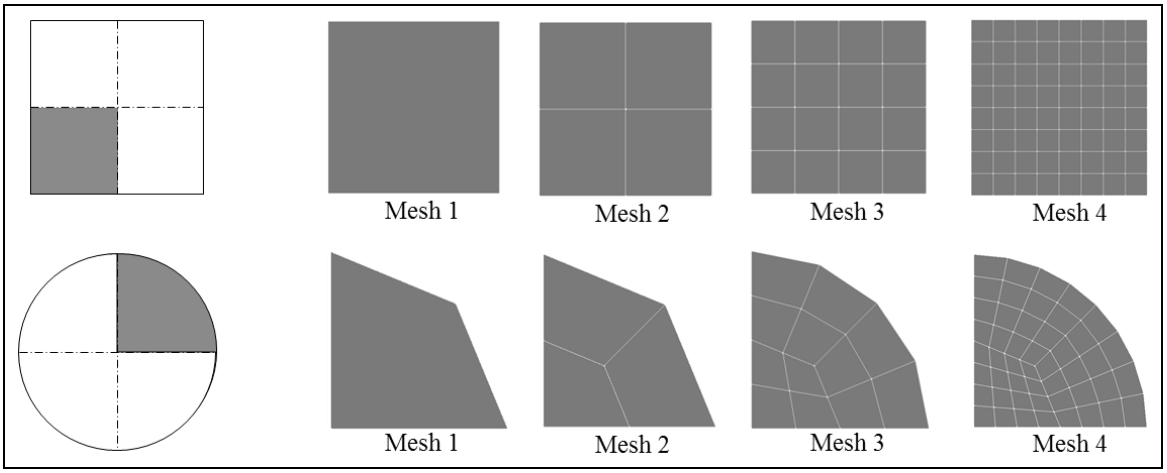

Figure 2. Mesh refinement parameter of the plates.

The second condition refers to reduced integration (R) for each element, also with reduced mesh size. Under this condition, the efficiency of the anti-locking integration was analyzed for thin plates, in addition to how it impacted the thick plate convergence.

For a comparison between numerical solutions and analytical solutions in this study, the maximum transverse displacement of the plates W_{max} was calculated according to Fig. 3.

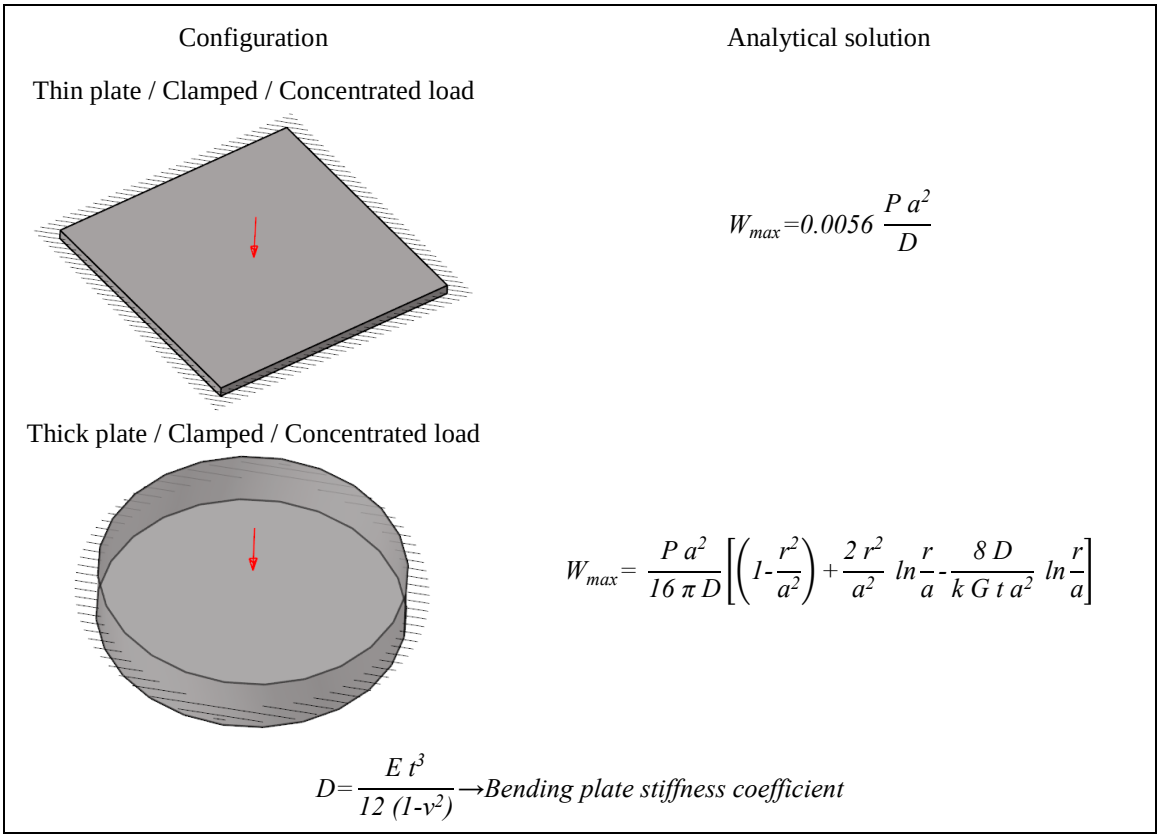

Figure 3. Analytical solutions for thin and thick clamped plates under concentrated load.

Figure 3 shows the thin plate equation as mentioned in Timoshenko and Woinowsky-Krieger (1959) and the thick plate, as found in Gruttmann and Wagner (2004). In both cases, the solutions depend on the load *P*, on the plate side or radio *a*, and on the parameter *D*, the Bending plate stiffness coefficient, which is formulated with the material properties and the plate thickness. Moreover, the solution for the thicker plate depends upon the shear modulus *G*, the shear correction parameter *k*, equal to 5/6, and the value of *r*, the center-to-point distance to be calculated (displacement). Once this variable was evaluated on the plate center, a value of *r=0.01 mm*, close to this place, was considered since singularity occurs for *r=0.00 mm.*

4. RESULTS AND DISCUSSIONS

The results and discussions are divided into three subsections. The first two contain a quantitative evaluation of the plate convergences and their respectively spurious modes. The last part summarizes the main investigation of the previous parts and adds a qualitative analysis of the computing time.

The convergence study is shown in graphics with the transverse displacement of the plates based on the mesh refinement for each element and integration condition. In addition, these values are presented in tables with the percentage difference (Δ%) from the numerical to the analytical solution in brackets. A negative sign in these differences means the obtained values are lower than the analytical ones and a positive sign means the opposite. An adequate percentage value treated in this work was around from – 5.0% to +5.0%.

The spurious modes are plotted in amplified scale factors of the transverse deformed shape with the Q4 elements and mesh 4. The full integration case is also included, for comparison against the result of a non-spurious mechanism. In all figures, the undeformed shape is presented in a wireframe mesh.

4.1 Thin plates

Figure 4 illustrates the convergence of the thin plate with the first integration condition.

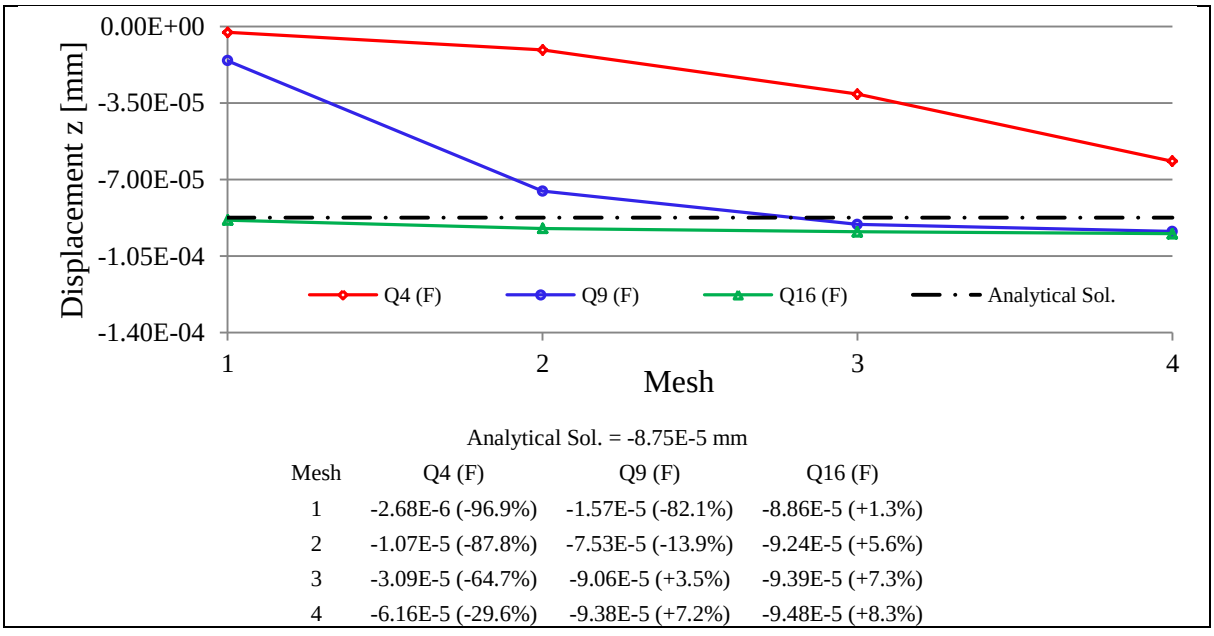

Analytical Sol. = -8.75E-5 mm

Mesh	Q4 (F)	Q9 (F)	Q16 (F)
1	-2.68E-6 (-96.9%)	-1.57E-5 (-82.1%)	-8.86E-5 (+1.3%)
2	-1.07E-5 (-87.8%)	-7.53E-5 (-13.9%)	-9.24E-5 (+5.6%)
3	-3.09E-5 (-64.7%)	-9.06E-5 (+3.5%)	-9.39E-5 (+7.3%)
4	-6.16E-5 (-29.6%)	-9.38E-5 (+7.2%)	-9.48E-5 (+8.3%)

Figure 4. Maximum transverse displacement and (Δ%) in the thin plate using full integration (F).

In thin plates using the Reissner-Mindlin theory with full integration, locking of the numerical solution is expected. It occurs with the Q4 element of the previous figure. However, by keeping this integration but increasing the element orders from linear to quadratic and cubic and refining their meshes (for quadratic element only), the numerical solution converges to the analytical one as presented in Fig. 4, with mesh 3 for the Q9 element and mesh 1 for the Q16 element. This convergence arises due to a significant increase in the degrees of freedom of the plate.

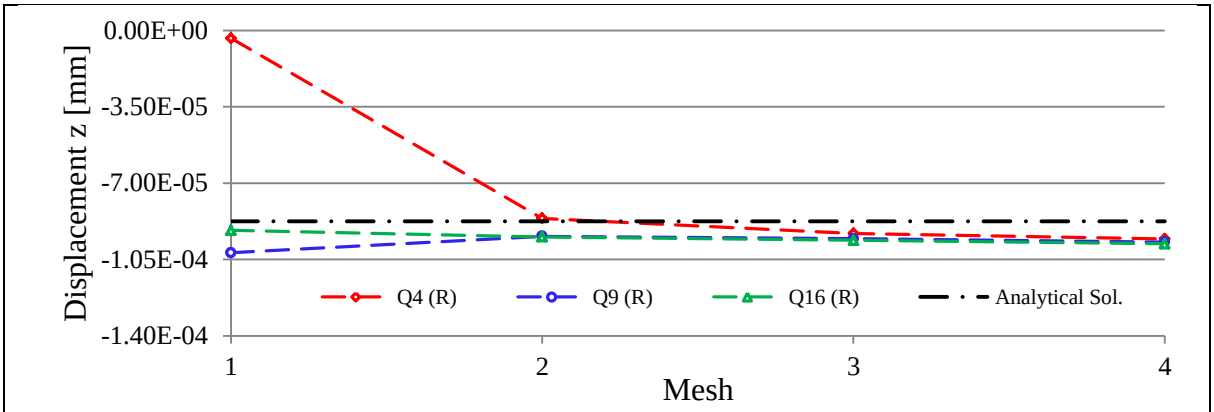

Analytical Sol. = -8,75E-5 mm

Mesh	Q4 (R)	Q9 (R)	Q16 (R)
1	-3.57E-6 (-95.9%)	-1.02E-4 (+16.5%)	-9.16E-5 (+4.7%)
2	-8.61E-5 (-1.6%)	-9.43E-5 (+7.8%)	-9.46E-5 (+8.1%)
3	-9.31E-5 (+6.4%)	-9.55E-5 (+9.1%)	-9.62E-5 (+9.9%)
4	-9.55E-5 (+9.1%)	-9.70E-5 (+10.9%)	-9.78E-5 (+11.8%)

Figure 5. Maximum transverse displacement and (Δ%) in the thin plate using reduced integration (R).

The second integration condition for this plate is displayed in Fig. 5. It is possible to notice the efficiency of the anti-locking technique especially with the Q4 element, where using mesh 2 alone led the percentage difference to vary from around -88% (F) to -2% (R).

Regarding reduced integration used in the same figure, a spurious mechanism shows at the plate deformation, the hourglass mode as detailed in Soriano (2003). This problem can be viewed in Fig. 6.

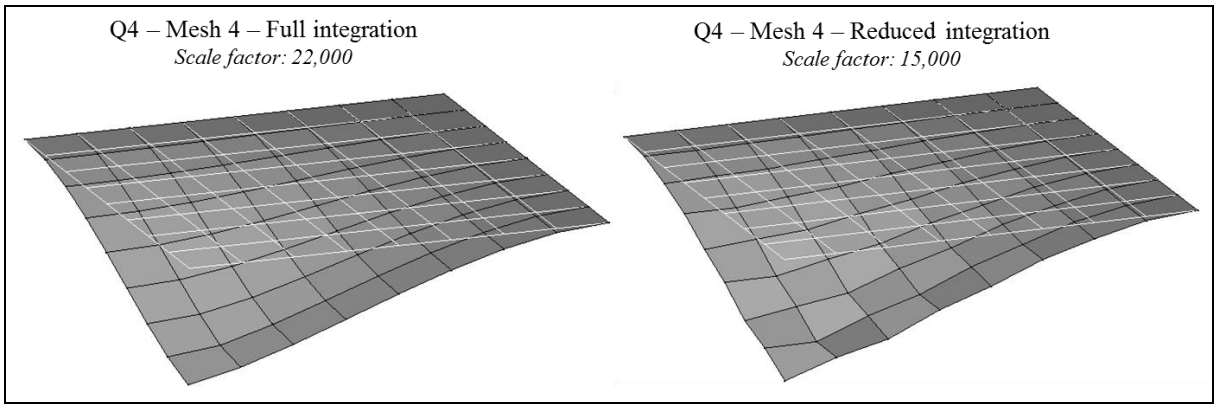

Figure 6. Hourglass mode in a thin deformed plate using reduced integration.

4.2 Thick plate

The first condition for the thick plate is shown in Fig. 7. It can be observed for this thickness where there is no locking that, the Q4 element tends to a better convergence than in the thin plate, when mesh size is reduced. Convergence becomes even better with the higher order elements.

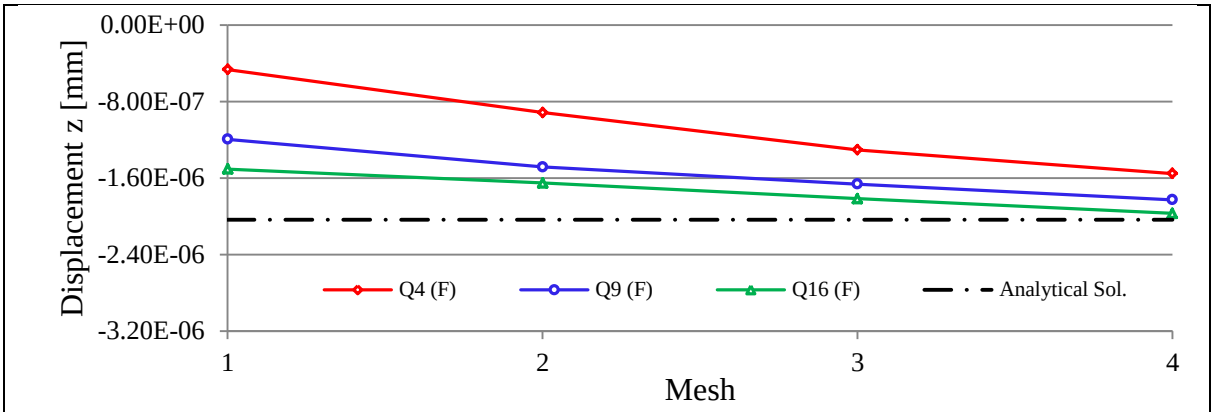

Analytical Sol. = -2.03E-6 mm

Mesh	Q4 (F)	Q9 (F)	Q16 (F)
1	-4.64E-7 (-77.2%)	-1.19E-6 (-41.3%)	-1.51E-6 (-26.0%)
2	-9.14E-7 (-55.1%)	-1.48E-6 (-27.1%)	-1.65E-6 (-18.9%)
3	-1.30E-6 (-35.9%)	-1.66E-6 (-18.3%)	-1.81E-6 (-10.8%)
4	-1.55E-6 (-23.7%)	-1.83E-6 (-10.2%)	-1.97E-6 (-3.2%)

Figure 7. Maximum transverse displacement and (Δ%) in the thick plate using full integration (F).

Lastly, the second condition for the thick plate is shown in the next figure.

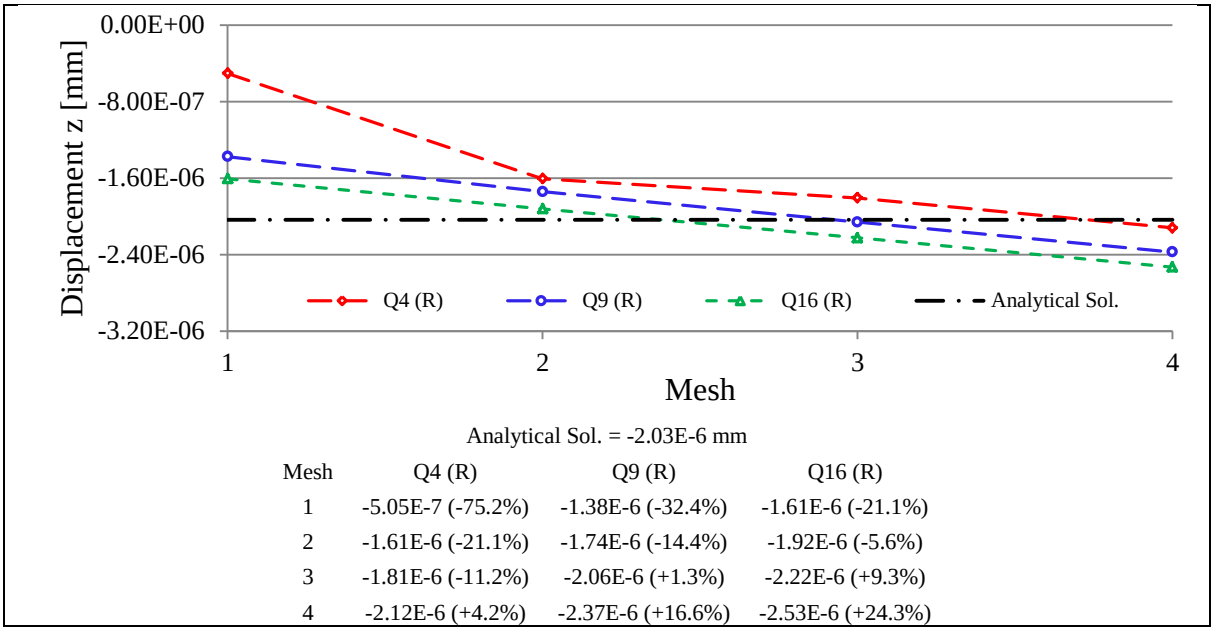

Analytical Sol. = -2.03E-6 mm

Mesh	Q4 (R)	Q9 (R)	Q16 (R)
1	-5.05E-7 (-75.2%)	-1.38E-6 (-32.4%)	-1.61E-6 (-21.1%)
2	-1.61E-6 (-21.1%)	-1.74E-6 (-14.4%)	-1.92E-6 (-5.6%)
3	-1.81E-6 (-11.2%)	-2.06E-6 (+1.3%)	-2.22E-6 (+9.3%)
4	-2.12E-6 (+4.2%)	-2.37E-6 (+16.6%)	-2.53E-6 (+24.3%)

Figure 8. Maximum transverse displacement and (Δ%) in the thick plate using reduced integration (R).

Figure 8 shows that reduced integration in the thick plates can provide extra flexibility, which can be used favorably in some situations, for example, commercial computer programs such as ABAQUS, in which the elements are available just up to quadratic interpolation. In this case, the Q4 and Q9 elements using reduced integration with mesh 4 and mesh 3, respectively, could be used instead of the Q16 element using full integration with mesh 4. However, special care must be taken to avoid excessive displacement with the Q9 element, as its value overtakes the analytical solution producing an error of +16.6%, as shown in mesh 4. It goes against a common practice in virtual analysis that says the lower the element size, the better is the result.

The hourglass mode in this integration and thickness could be noticed again but with a difference in the thin plate: the spurious mechanism propagated in the mesh, according to Fig. 9.

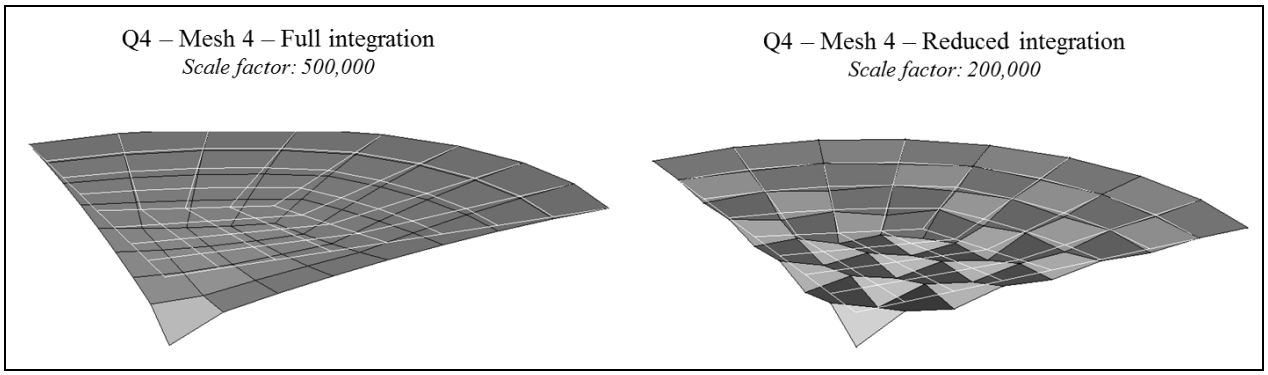

Figure 9. Hourglass mode in a thick deformed plate using reduced integration.

4.3 Summary of the study

Summing up the research, Tab.1 outlines the results and gives alternative paths to convergence in thin and thick plates with different performances for spurious mode and time. This last variable was considered in a qualitative form. Since reduced integration provides fewer points to be computed in the element stiffness matrix, this condition takes up less time, in relation to full integration.

In this way, these variables are compared individually and qualitatively by using the symbol ↑ meaning a superior result compared to ↓.

Table 1. Summary of the main investigations in the study.

Analysis	Integr.	Thickness	Element	Conv.	Spurious Mode	Time
1. Full integration (F) in thin plates, alternative to reduced integration (R)	(R)	Thin	Q4	↑	↓	↑
	(F)		Q9, Q16	↑	↑	↓
2. Reduced integration (R) in thick plates, alternative to full integration (F)	(F)	Thick	Q16	↑	↑	↓
	(R)		Q4, Q9	↑	↓	↑

5. CONCLUSION

The study presented in this paper about finite element plates based on the Reissner-Mindlin theory verified, by means of convergence analyses, the efficiency of the anti-locking technique for a thin plate, especially with a linear element. It also provided an alternative to this technique, using higher order elements with full integration and small dimensions.

This work also investigated another possibility, reduced integration in thick plates combined with lower order elements, for cases in which higher order elements with full integration are impracticable.

All these alternatives are shown in Tab.1 and with distinct meshes, reached basically the same acceptable convergence percentage difference, resulting in different element orders and integrations. Reduced integration is the type that takes the lowest computing time, despite the generation of hourglass spurious mode to both thickness cases. Said problem does not occur if full integration is used, but a longer time in the numerical solution of the problem is necessary. Therefore, for the thin and the thick plate, these convergence procedures deliver an advantage and a disadvantage. A proper balance that focuses on the absence of spurious mechanism or in less time is helpful to decide which is the best choice in each simulation to be run.

6. REFERENCES

Cen, S. and Shang, Y., 2015. “Developments of Mindlin-Reissner plate elements”. Hindawi Publishing Corporation, Beijing, 12p. 29 Sep. 2018 <http://dx.doi.org/10.1155/2015/456740>.

Gruttmann, F. and Wagner, W., 2004. “A stabilized one-point integrated quadrilateral Reissner-Mindlin plate element”. *International Journal for Numerical Methods in Engineering*. 09 Dec. 2018 <https://doi.org/10.1002/nme.1148>.

Oñate, E., 2019. *Structural Analysis with the Finite Element Method. Linear Statics. Vol.1. Basis and Solids*. Springer, Barcelona, 1st edition.

Oñate, E., 2013. *Structural Analysis with the Finite Element Method. Linear Statics. Vol. 2. Beams, Plates and Shells.* Springer, Barcelona, 1st edition.

Saliba, S. S., 2007. *Implementação computacional e análise crítica de elementos finitos de placas*. Dissertação de Mestrado, Universidade Federal de Minas Gerais, Belo Horizonte, Brasil.

Soriano, H. L., 2003. *Método de elementos finitos em análise de estruturas*. Edusp, São Paulo, 1st edition.

Timoshenko, S. and Woinowsky-Krieger, S., 1959. *Theory of Plates and Shells.* McGraw-Hill Book Company, New York, 2nd edition.

7. RESPONSIBILITY NOTICE

The authors are the only responsible for the printed material included in this paper.